J. Mar. Biol. Ass. U.K. (2003), **83**, 673–682
Printed in the United Kingdom

Heat, salt and tracer transport in the Plymouth Sound coastal region: a 3-D modelling study

J.R. Siddorn*, J.I. Allen and R.J. Uncles

Plymouth Marine Laboratory, Prospect Place, Plymouth, PL1 3DH. *Corresponding author, e-mail: john.siddorn@metoffice.com
Present address: The Hadley Centre for Climate Prediction and Research, The Met Office, London Road, Bracknell, RG12 2SY

A 3-D hydrodynamic model of the circulation, salinity and temperature within the embayment of Plymouth Sound, UK and its surrounding English Channel waters has been implemented. Thorough validation of the model shows that the main hydrographic features of the region, as characterized by these variables, are reproduced. The general flow characteristics, and the resultant distribution of freshwater from the main riverine source (the River Tamar), are described. The potential fate of contaminant releases within Plymouth Sound is investigated. Whitsand Bay, located south-west of Plymouth Sound, is shown to be a likely recipient for a proportion of these contaminants, irrespective of where in the Sound the release occurs, and as such is considered to be vulnerable to pollution events originating there.

INTRODUCTION

The aim of this work has been to implement a model of the circulation of water, salt and heat in the coastal waters offshore of the city of Plymouth, UK, as a framework for future biogeochemical and sediment modelling work. There have been successful modelling studies of the riverine end of the system, using laterally averaged models (Uncles & Stephens, 1990; Harris et al., 1991), but there have been no attempts known to us to model the coastal processes of the region. Conceptually, this work is envisaged as a link between 3-D basin scale models (Holt et al., 2001) and fine-scale, estuarine and riverine models.

The model domain extends from English Channel coastal waters of about 70 m depth in the south to the mouth of the River Tamar in the north, including Plymouth Sound (Figure 1) which has a maximum width of 6 km, and a mouth that is approximately 5 km wide. The main features of the Sound are Plymouth Breakwater, a construction built in the early 19th Century and situated roughly in the centre of the Sound, Drake's Island, and the rivers Tamar and Plym. Drake's Island is situated at the mouth of the Tamar and is separated from the Cornish mainland by the shallow Bridge Channel. These features act to constrain the flow of freshwater into the Sound. The River Tamar is the main source of freshwater, with an average freshwater flow ranging from 5 $m^3 s^{-1}$ to 140 $m^3 s^{-1}$ (Uncles & Stephens, 1990), compared with an average flow of approximately 1 $m^3 s^{-1}$ from the Plym. There is a main channel, maintained by dredging, that flows from the mouth of the Tamar (the Narrows) past the north of Drake's Island and around the eastern side of the Sound. It splits north-east of the Breakwater to form two channels, the Eastern and Western Channels.

This paper investigates the ability of a modelling system to reproduce the hydrodynamic features of Plymouth Sound (at relatively coarse resolution) and, especially, the surrounding coastal waters. The L4 site, situated approximately 10 km offshore at 50°15′N 04°13′W, has been sampled regularly since 1985 (and more sporadically prior to that) for biological data, and will provide a focus for future biogeochemical modelling studies. There are also surface temperature and salinity data available for the site. Other, less frequently sampled sites also exist, although the amount of hydrographic information is limited. Biological studies (e.g. Laabir et al., 1998; Biegala & Harris, 1999; Irigoien et al., 2000) have, therefore, relied on limited information about the physical environment. Any future biological work would benefit greatly from an improved understanding of physical processes in the area in general, and particularly at these sites. Also, understanding the transport of discharged material in the area is of scientific and public interest. For example, there are concerns about the impacts of dredging and the potential impacts of radiochemical discharges in the River Tamar.

MATERIALS AND METHODS

The model domain extends from 50°05′ to 50°22′N and from 04°20′ to 04°03.8′W (Figure 1), divided into cells of dimension 1/240° latitude and 1/150° longitude (approximately 500 m by 500 m) and 20 levels in the vertical. In the vertical a sigma grid is used; each horizontal grid point has 20 equally spaced vertical points, giving a vertical resolution of less than 50 cm in the shallower areas and more than 3 m in the deeper offshore regions. Corrections for erroneous horizontal pressure gradients that can be created by the use of sigma-levels in steep topography are included, making this model ideal for the steep topography and large density gradients of the Plymouth Sound region.

The region contains a number of features that, due to their scale, have had to be dealt with carefully. The Eddystone Rocks, which protrude above the sea surface, have been modelled as a pair of adjacent, relatively shallow (10 m) cells. The topography between the mouth of the Tamar and Drake's Island is resolved only poorly

https://doi.org/10.1017/S002531540300763Xh Published online by Cambridge University Press

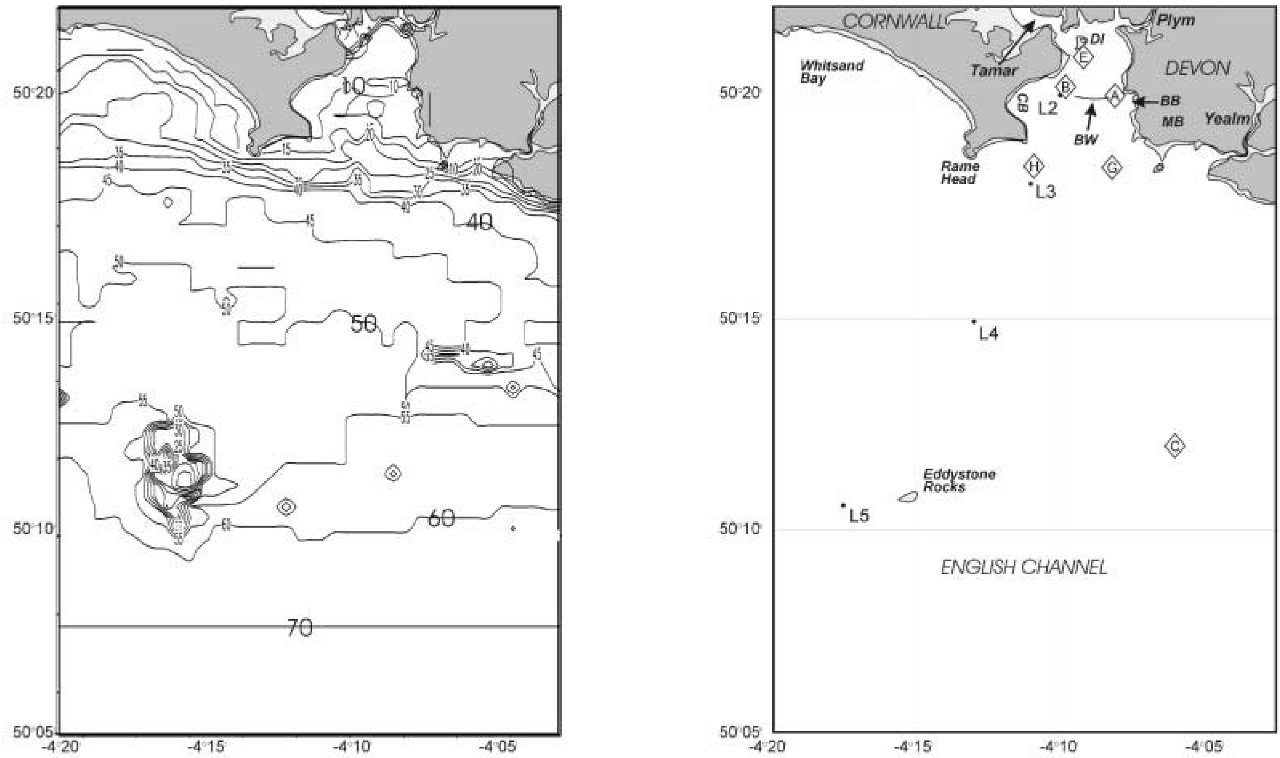

Figure 1. Map of the domain showing, on the left, the bathymetry and on the right some of the region's main features. Sampling sites, L5, L4, L3 and L2, and sites of admiralty tidal diamonds are marked and major geographical features are labelled, with abbreviations BB, CB, DI, MB and BW referring to Bovisand Bay, Cawsand Bay, Drake's Island, Mountbatten and the Breakwater respectively.

in the model, so that the simulated circulation cannot be considered an accurate representation of the actual flow there. However, care has been taken to ensure that the majority of the flow is constrained to the channel north of Drake's Island, with a smaller transport allowed across the Bridge Channel. The other major feature of the region is the Breakwater, which is approximately two kilometres long and is approximated by a single line of non-active cells. The bathymetry of the domain was estimated from Admiralty Charts of the region.

The model uses the POL3DB code (Proctor & James, 1996), a three-dimensional finite difference primitive equation model. This is capable of dealing with the high spatial and temporal gradients associated with fine-scale topographic and hydrodynamic variability, and has previously been coupled with the European Regional Seas Ecosystem Model (ERSEM) (Allen et al., 2001), making it ideally suited for future biogeochemical studies.

Lateral boundary conditions

Temperature and salinity

At the boundaries the scalar properties are treated using an upstream advection condition (e.g. Palma & Matano, 2000). For flow into the model domain across the boundaries:

$$X = X + \frac{\Delta t}{\Delta x}\left[\bar{U}(X_{BC} - X)\right] \qquad (1)$$

where X is the computed value for the scalar at the boundaries, X_{BC} is the prescribed data value for the boundary, and is the water speed normal to the boundary. Δt and Δx are the timestep and horizontal grid resolution respectively. Similarly, for flow out of the domain:

$$X = X + \frac{\Delta t}{\Delta x}\left[\bar{U}(X_{+} - X)\right] \qquad (2)$$

where X_{+} is the grid cell adjacent to the boundary cell and normal to the boundary.

Data from a laterally averaged model of the Tamar (Uncles & Stephens, 1990) are used as the boundary condition for the open cells in the north, and data from the E1 monitoring station (50°02′N 04°22′W, approximately 4 km south-west of the south-western corner of the model domain) are used for the southern boundary. Ideally measurements at a resolution comparable to the grid size of the model or failing this data from a larger area model would be available. However, these measurements are not available and tests show that due to the strong longitudinal gradients in salinity and temperature the interpolation, and extrapolation, of relatively course data to the model grid results in spurious inputs of both heat and salt at the boundaries. It was thus found that the model performed best where no temperature or salinity data was supplied at the east and west boundaries, but the external temperature and salinity boundary conditions were given equal to the internal value. Thus for flows into the model domain the value is unchanged (eqn 1 is in effect defunct as X_{BC} is

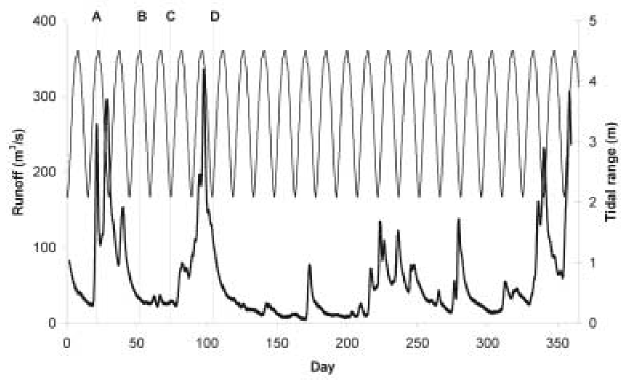

Figure 2. Freshwater run-off from the River Tamar, tidal range at the mouth of the Tamar and the timing of the four scenarios, labelled A—springs, high run-off; B—springs, low run-off; C—neaps, low run-off; D—neaps, high run-off.

equal to X), but for flows out of the domain eqn 2 still applies.

Velocity and elevation

The boundaries are forced in the east, south and west by the M2 and S2 tidal constituents for velocity and elevation obtained from an approximately 5 km resolution shelf seas tidal model (Pingree & Griffiths, 1980; Sinha & Pingree, 1997) using a flux/radiation boundary condition, the flux component of which is the volume flux into, or out of, the domain due to the boundary data tidal velocities at, and normal to, the boundary. The total depth mean current used to calculate boundary elevations is the sum of these fluxes plus, for normal components, the radiation term, which is the flow into the domain due to the surface slope (simply the difference between the model elevation and the boundary elevation data) travelling at the speed of a shallow water wave.

For the northern boundary, where there is the Tamar freshwater inflow, the same boundary condition is applied without the inclusion of the radiation term, but including an additional flow due to the volume run-off from the Tamar (Figure 2). The run-off data used is daily averaged, and was derived from *in situ* velocity measurements taken by South West Water. The M2 and S2 tidal constituents were extracted from the output of a one-dimensional tidally averaged model (Uncles & Stephens, 1990). The shelf seas tidal model data, which is not referenced in time, is temporally shifted for consistency with these Tamar elevations and velocities.

Surface and bottom boundary conditions

Wind stress is calculated using the quadratic drag law following the standard parameterization for the coefficient of drag of Smith & Banke (1975). Bottom stress is also calculated using standard parameterizations following Ruddick et al., 1995. The surface temperature is determined by empirical formulations for the latent heat of evaporation (L_E), short-wave back radiation (L_S) both from Kondo (1975), and the long wave solar radiaton (L_R) from the

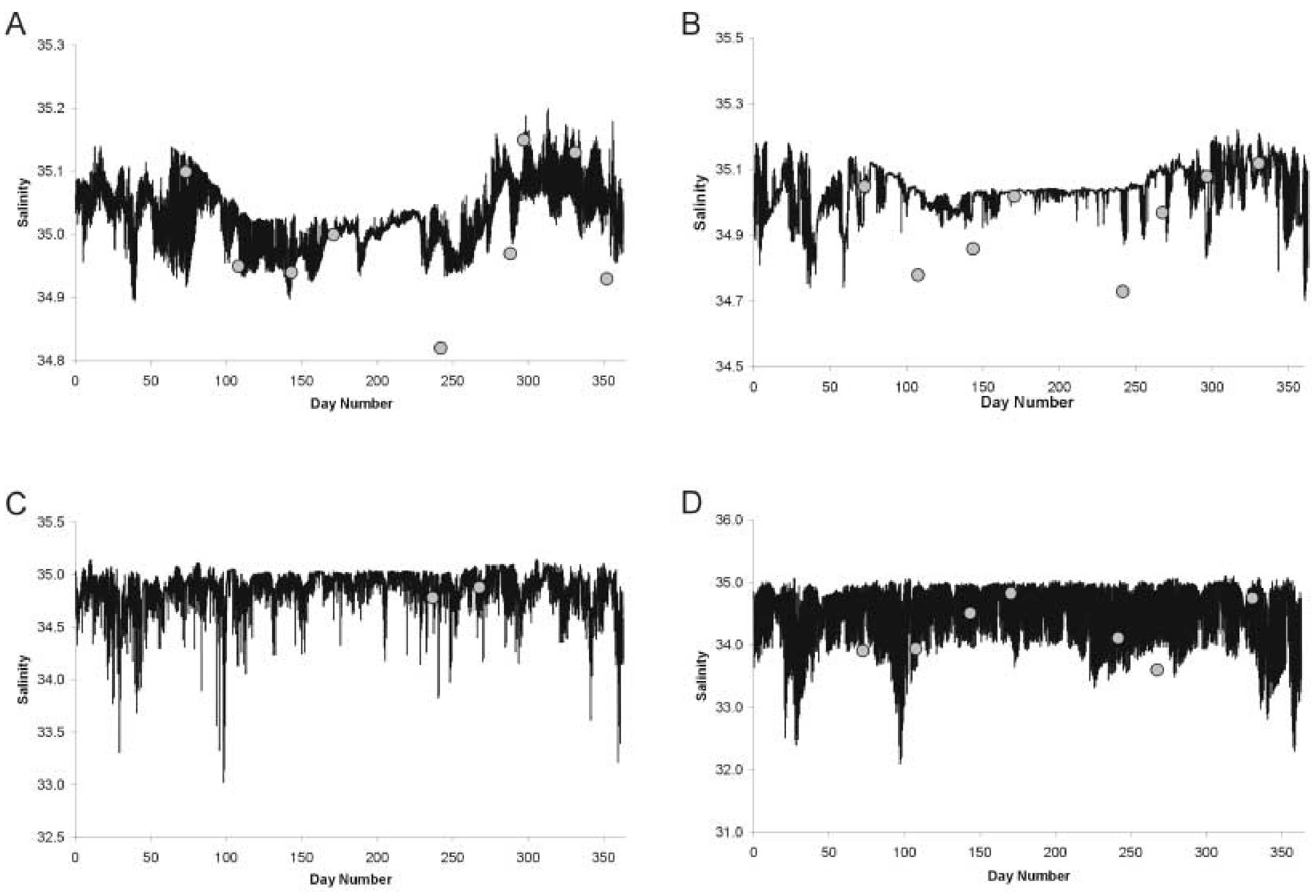

Figure 3. Modelled (line), and *in situ* measured (solid grey circles) surface salinities for sites (A) L5; (B) L4; (C) L3; (D) L2.

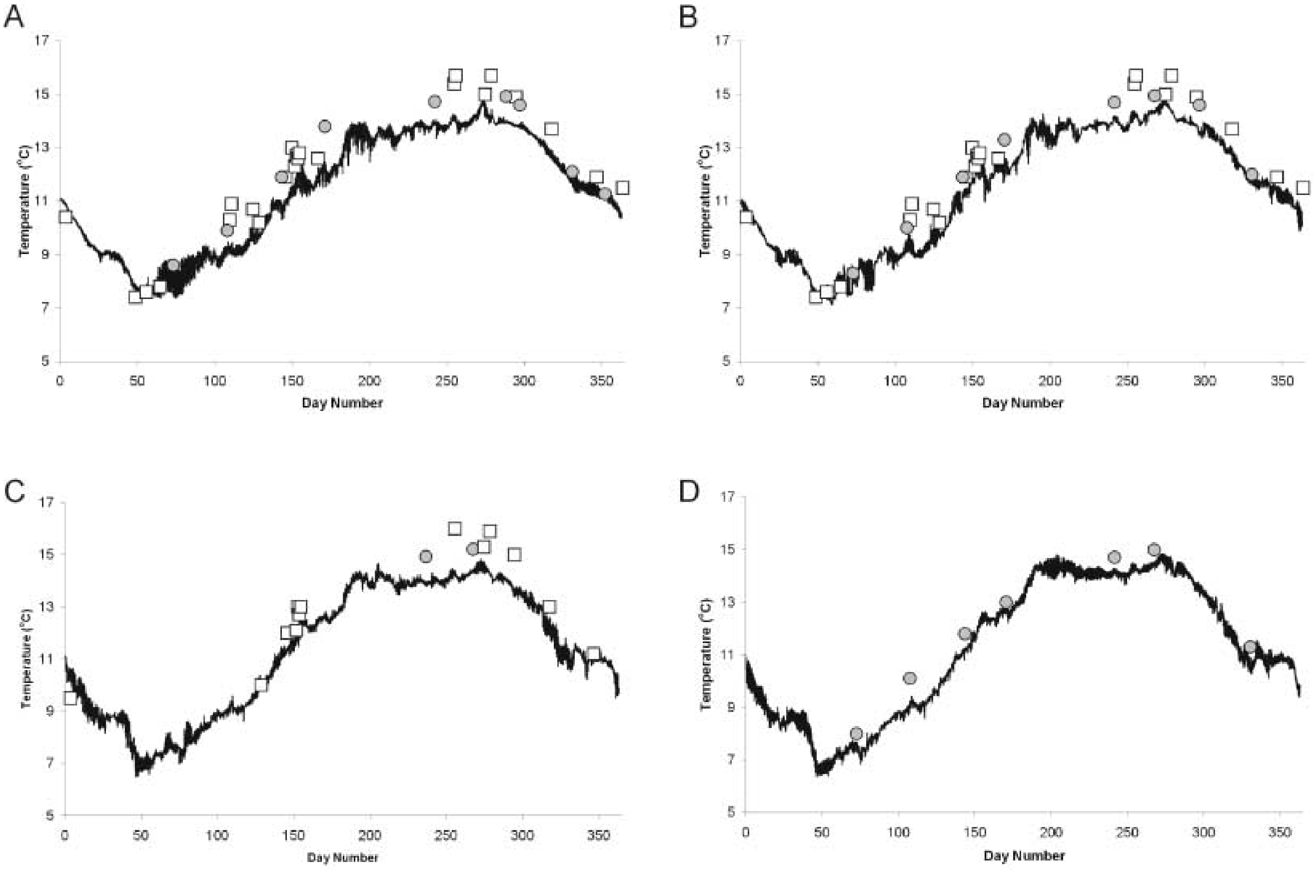

Figure 4. Modelled (grey line), *in situ* measured (solid circles) and AVHRR (empty squares) surface temperatures for sites (A) L5; (B) L4; (C) L3; (D) L2.

May formulation (Budyko, 1974) using transfer coefficients calculated from Kondo (1975), and hourly meteorological data obtained from the Mountbatten meteorological station (Figure 1). Evaporation and precipitation are not explicitly considered as part of the salt budget although are implicitly included due to the impacts they have upon the river inputs and seaward boundary salinities.

A 12 month 'spin-up' period, driven by 1985 meteorological and physical forcing data (detailed previously), was used to provide realistic initial conditions. All results shown are for an annual run, beginning on the 1 January 1985 using this initialization and forced by the same data. Four periods from this run have been highlighted, a spring tide with high river run-off, a spring tide with low river run-off, and similarly neap tides with both high and low run-off. The timing of these events are shown in Figure 2.

RESULTS

Model validation

Temperature and salinity

There are four monitoring sites (L5, L4, L3 and L2) within the model domain (Figure 1) at which surface temperature and salinity data are available. The modelled surface temperature and salinities are compared with available *in situ* data from 1985. This comparison shows the modelled temperature has quite a strong negative bias, having a mean error of -0.68°C (standard deviation 0.38°C). The salinity does not show such a consistent bias, although does have a mean error of 0.11 (standard deviation 0.42).

The precise time of sampling (other than the date) is unspecified for these data and so it is assumed to have been collected at midday. Given that both salinity and temperature show marked diurnal variations exact comparisons between the data and the model are difficult to make. The strong diurnal signal in the salinity in particular may account for a large amount of the error, with a mean diurnal salinity range of 0.37 being comparable with its standard deviation. Time-series plots show that the salinity is consistent for all but a small number of points (Figure 3), but the temperature is consistently underestimated, especially in the summer (Figure 4). The strong fluctuations in salinity are associated with events of high river run-off for the offshore sites (L2 and L3) but for sites within and close to the Sound run-off plays a lesser role (Figures 2 & 3), with tidal and to a lesser extent wind mixing determining stratification and thus the mixing out of freshwater. Figure 4 shows the temperature stratification at the site L4, and indicates that the site is stratified throughout the summer months, with as much as a two degree difference between the surface and bottom waters.

Velocity

There is little data in the Plymouth coastal region, but crude tidal velocities for spring and neap tides available from Admiralty Charts 'diamonds' (so called as the

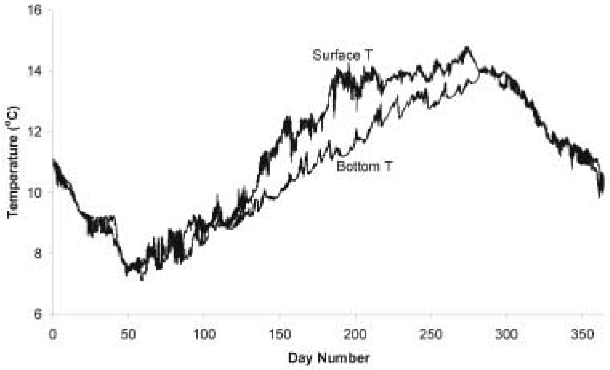

Figure 5. Surface and bottom temperatures at the site L4.

position of the data is marked by a 'diamond') (Figure 1), have been used to give a semi-quantitative validation of the model velocity fields (Figure 6). These show that the model produces current magnitudes and directions of the right order.

Current fields

Surface current fields for a spring tide with low run-off from the River Tamar are shown in Figure 7. There are two main features of the flows in the Plymouth Sound coastal region, the increased velocities around the Eddystone Rocks and the two currents that flow to the west and east of the Breakwater, turning to the west as the tide progresses and eventually converging to flow into Whitsand Bay.

Three hours before high water at the mouth of the Tamar (Figure 7A), the waters have begun to flood, especially in the Sound where flows of up to 1.2 m s^{-1} occur north of the Breakwater. The flow in English Channel coastal waters is largely quite slack, except around the Eddystone Rocks with currents of up to 0.7 m s^{-1}. At high water (Figure 7B) there is a general flow to the east of approximately 0.5 m s^{-1}, reaching as much as 0.8 m s^{-1} around the Eddystone Rocks. Three hours later, at mid water on the ebb tide (Figure 7C), the offshore currents have slackened and begun to turn more southerly and westerly, whilst the flows within the Sound reach their maximum with southerly flows of up to 1.3 m s^{-1} through the channel west of the Breakwater and up to 1.1 m s^{-1} through the eastern channel. There is a large region south, and in the lee, of the Breakwater where the flow is less than 0.1 m s^{-1}. At low water (Figure 7D), a further three hours later, the main flows from either side of the Breakwater have turned westerly, and to some extent converged, with the fastest waters being located further to the south and west around the Rame Head peninsula. This water flows into Whitsand Bay at speeds of up to 1 m s^{-1}. Offshore, the currents run mainly east to west at speeds of 0.4 m s^{-1}, reaching a maximum of 0.8 m s^{-1} around the Eddystone Rocks.

This tidally dominated pattern of water movement is also evident for neap tides, where the general patterns shown in Figure 6 also apply, although the velocities are smaller. The maximum flows found in the Sound at both flood and ebb mid waters are of the order of 1.2 m s^{-1} at springs but rarely go above half of that on a neap tide. Similarly, the flow around Rame Head at low water is substantially greater on springs than neaps (maximum of above 1 m s^{-1} compared with 0.6 ms^{-1}).

It was found that the flow was not significantly different from that described above for periods of high run-off from the River Tamar, except for immediately adjacent to the river boundary cell.

Freshwater flows

The dispersion of freshwater in coastal areas is vital to our understanding of the physical and biological processes in the region. It indicates the possible fate of terrigenous matter in coastal waters, which in turn may influence the biology of the system. Modelled surface salinity, as an indicator for freshwater influence, and how it is affected by changes in state of tide and run-off characteristics are investigated. Runs were also undertaken with changed meteorology, but the meteorological influence was found to be small and so the results are not shown.

Four scenarios were investigated to compare the effects of tides and river run-off, a spring tide with high river run-off, a spring tide with low river run-off, and similarly neap tides with both high and low run-off (Figure 2). A similar pattern of salinity distribution is seen for all of the scenarios. However, the relative

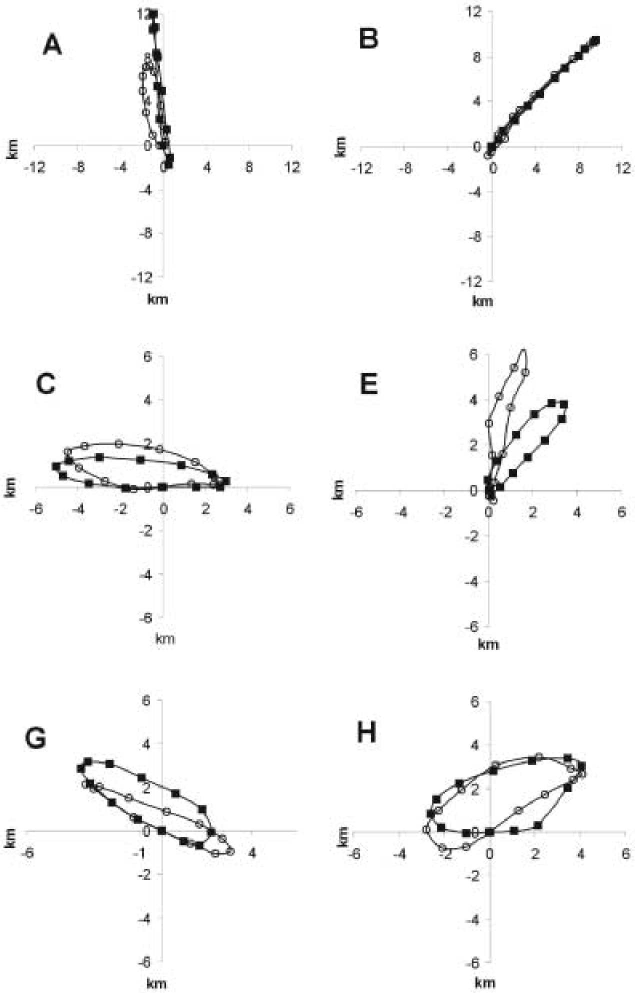

Figure 6. Admiralty (open circles) and modelled (closed squares) tidal ellipses for tidal diamonds from Admiralty Charts 1613 (diamonds C, G and H) and1967 (diamonds A, B and E). The residual flows are removed in both cases.

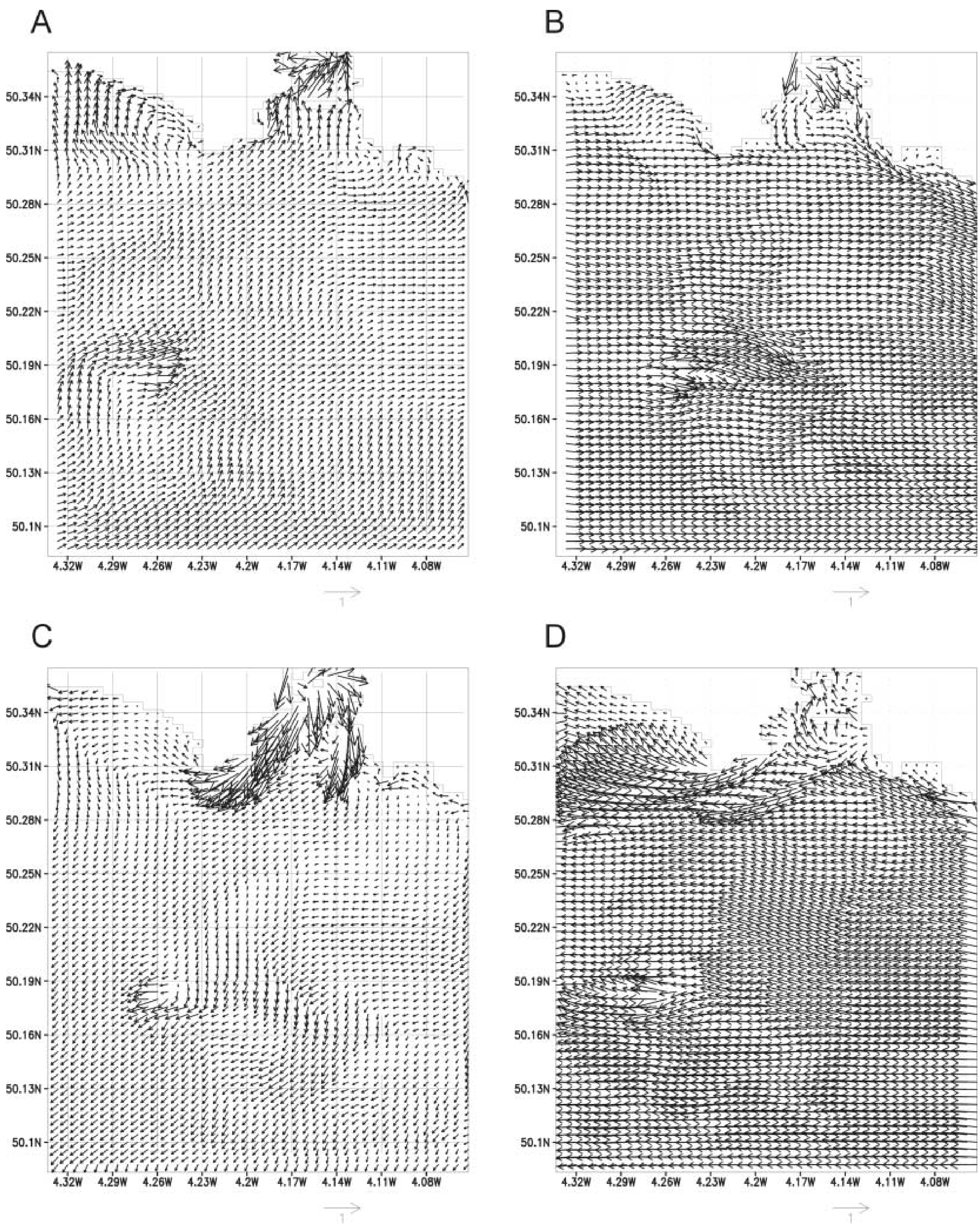

Figure 7. Surface currents (m s^{-1}) for (A) three hours before high water at Devonport (near the mouth of the Tamar); (B) high water; (C) three hours after high water; and (D) low water.

influence of the Tamar run-off upon the coastal waters varies depending upon the tidal range and strength of run-off. At neap tides, significantly less of the plume is transported around Rame Head and the freshness of this transported water is heavily influenced by the strength of run-off.

To illustrate the salinity distribution the high run-off, spring tide scenario is shown in Figure 8. This shows that

https://doi.org/10.1017/S002531540300763Xh Published online by Cambridge University Press

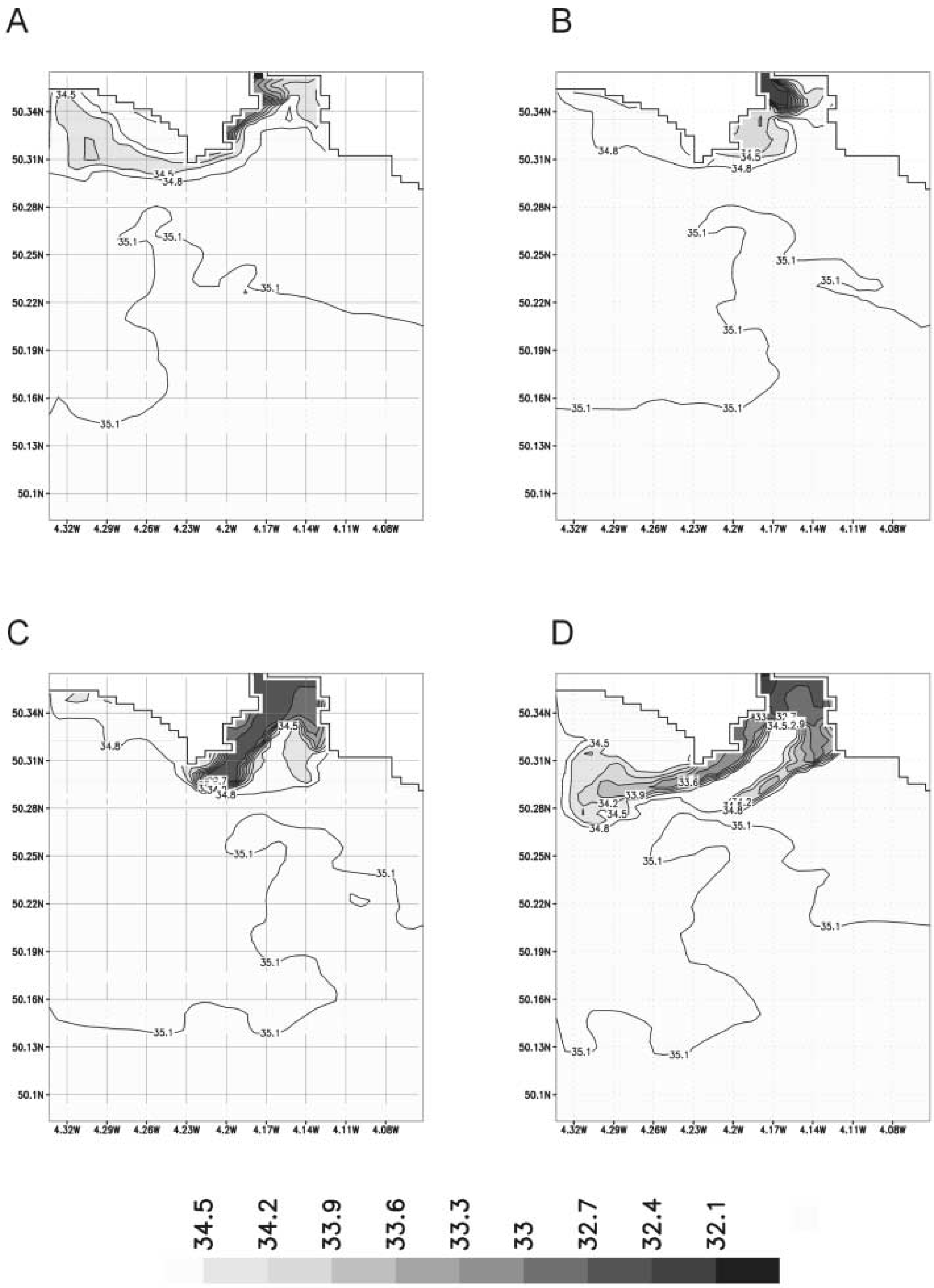

Figure 8. The surface salinity fields for (A) three hours before high water at Devonport (near the mouth of the Tamar); (B) high water; (C) three hours after high water; and (D) low water.

at high water (Figure 8B) the freshwater is restricted by the incoming tide to the north-western corner of the Sound around Drake's Island. There is also a patch of low salinity waters in Cawsand Bay, resulting from a combination of the return of the freshwaters transported around Rame Head on the previous tide and the trapping of low salinity waters in the bay. Some remnants of the low salinity water transported on the previous tide can also remain in Whitsand Bay. As the tide ebbs it carries freshwater from the Tamar with it, through the East and West Channels, and past the Breakwater. Although the flow speeds are similar through these channels (Figure 7C),

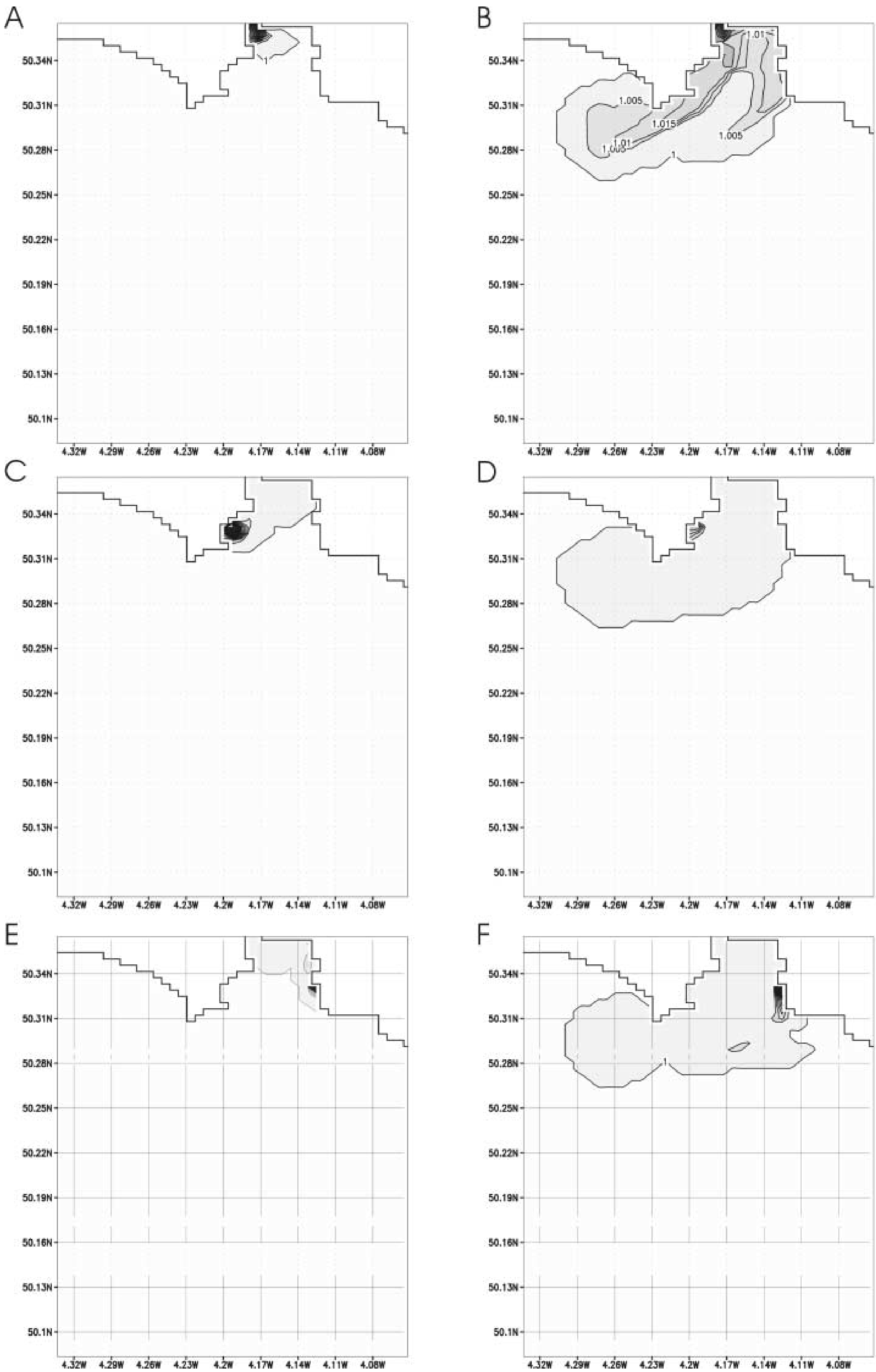

Figure 9. The surface tracer distribution for (A) high water at Devonport (near the mouth of the Tamar), six hours after release in the River Tamar; (B) low water, 12 hours after release in the River Tamar; (C) high water, six hours after release in Cawsand Bay; (D) low water, 12 hours after release in Cawsand Bay; (E) high water, six hours after release in Bovisand Bay; and (F) low water, 12 hours after release in Bovisand Bay.

https://doi.org/10.1017/S002531540300763Xh Published online by Cambridge University Press

the majority of the freshwater is transported through the West Channel as a surface flow, with the plume extending beyond Rame Head by the time mid water on the ebb is reached (Figure 8C). This plume extends further south and west as low water approaches (Figure 8D), and becomes concentrated along the coast in Cawsand Bay, where it extends in a narrow tongue approximately 10 km west and slightly south from Rame Head. There is also a second, smaller tongue of freshwater, extending south of the East Channel, which has developed by this stage. As the tide turns to the north and begins to flood (Figure 8A) much of the freshwater that has travelled beyond Rame Head remains in Whitsand Bay, whilst in the approaches to the Sound the plume is reduced to a narrow band of freshwater in Cawsand Bay and near the mouth of the Tamar.

Tracer

Releases of an arbitrary amount of a tracer (10 $kg\,s^{-1}$) into the surface waters at three sites, the mouth of the Tamar, Cawsand Bay and Bovisand Bay (Figure 1) were simulated. The releases were started at low water for the high run-off spring tide scenario (Figure 2) and the model run through to the following low water using a continuous source of the tracer. The runs were initialized with a background level of tracer of 1 $kg\,m^{-3}$.

Figure 9 shows the surface dispersion of the material at high water (six hours after the release was initiated) and at the following low water for the three release sites. At, and up until, high water high concentrations of the tracer can be found near the source, and, although there is some dispersion into the Sound, the levels found elsewhere are close to the initial background level of 1 $kg\,m^{-3}$. This is especially the case for the period before high water, where the flow is almost entirely into the Sound and acts to constrain the dispersion of the tracer. At high water, however, the tide begins to turn, which in the case of the Tamar release begins to carry the tracer southwards into the Sound; the two other tracer experiments show no southward transport at this stage, but the turning of the tide allows the transport of the tracer into the area of the Sound north of the Breakwater.

Soon after high water the tide begins flowing predominantly to the south and begins to significantly disperse the tracer inputs. This is especially true of the release implemented in the mouth of the Tamar, where the tracer is carried through both East and West Channels, turning to the west around Rame Head (much as the freshwater flowing from the Tamar does, Figure 8) and eventually some of this material becomes trapped in Whitsand Bay on the returning tide. The releases on either side of the Sound do not get carried out of the Sound in such large quantities, presumably because in both these cases the sources are in slow-flowing water outside the main channels (Figure 9D,F). In fact, the release on the eastern side of the Sound shows quite significant build up at the point of input, even during the ebb tide. The release in Cawsand Bay shows less build up at the point of input, but, unlike the Tamar release, which gives rise to a substantial plume of high concentration (Figure 9B), the dispersed tracer seems to be well mixed and doesn't give rise to substantially elevated concentrations in any particular region. Importantly, all three releases eventually give rise to some trapping of the tracer in Whitsand Bay.

It is evident, therefore, that should there be a release of an inert contaminant somewhere within the confines of Plymouth Sound the transport of the contaminant, and its subsequent dilution, will depend upon the site of the release. Releases directly in the main flows give rise to plumes of substantially elevated concentrations in the surface waters, whereas in sheltered regions the local effect may be greater. Wherever the release, though, some of it will eventually end up in Whitsand Bay.

DISCUSSION

A three-dimensional baroclinic model of Plymouth Sound and the surrounding area has been implemented on a 500 m grid. The model shows good agreement with available data, although the measured velocity fields are poorly documented and the comparison with Admiralty tidal data is not ideal. The only other publicly available source of information on the area's tidal currents in the detail required for these purposes is from a descriptive account written more than a century ago (Inglis, 1877) which gives a detailed, although rather impenetrable, account of the currents, the main features of which are evident in the flows shown by the model.

Salinity and temperature data are more readily available, and the model has been shown to reproduce the main features of these data satisfactorily. However, the validation of the temperature fields shows an underestimation of the summer surface temperatures throughout the model domain (Figure 4). Surface temperatures in the summer months are dependent, to a large extent, upon the surface heat flux from/to the atmosphere. Different empirical heat flux formulations used in ocean/coastal modelling have been shown to give rise to significant differences in temperature characteristics of a 3-D coastal model of the Mediterranean Sea (Castellari et al., 1998). The choice of heat flux formulation in this modelling study would be expected to be important in determining the surface temperature fields. Using a number of the formulations proposed by Castellari et al. (1998) in this work resulted in, to a lesser or greater extent, an underestimation of the surface temperature. Siddorn & Allen (2002) showed that the frequency of meteorological forcing data could have an effect upon heating in a 1-D model. There is the possibility that the diurnal thermocline in the summer months is not being adequately resolved by the vertical resolution of the model, leading to this underestimation. Excessive diffusion due to the vertical mixing scheme may also be a cause of underestimating surface temperatures. Further work is needed to determine whether the problem lies with one or more of the heat flux, the vertical resolution or deficiencies in the vertical mixing scheme.

The modelled salinity more closely matched observed values (Figure 3) but also showed some discrepancies between the data and model. Most noticeably, the *in situ* measured data shows an episode of substantial offshore transport of freshwater at around day 240, which is not reflected in the model results. This may be due to the high spring tides that occur around the equinoxes but which are not reflected in the tidal forcing used, the model being forced with M2 and S2 data which combine to give the spring–neap cycle but not the longer period variations in tidal amplitude.

Freshwater input from the River Tamar is fed into the system in the form of river flow and salinity values, which are taken from a one-dimensional, laterally averaged model of the Tamar (Uncles & Stephens, 1990). No other freshwater sources are explicitly included, although diffuse inputs are implicit from the seaward boundary salinity and temperature variations. This seaward data (taken from station E1 in the English Channel) is, however, sparse; the boundary information is interpolated between data of approximately monthly resolution, and so many short-lived changes in coastal-zone salinity will be missing from the model. Inclusion of the rivers Plym and Yealm may also make some difference, although the Tamar dominates freshwater inputs to the system. Despite these shortcomings, in general the validation of the model can be considered good, given the constraints of modelling such a complex, open-boundary system.

An important result for the local scientific community has been the modelled impact that the Tamar outflows have on the waters at the L4 monitoring site (Figure 1), which were previously considered to be uninfluenced by local riverine inputs. Instead, it has become apparent that the L4 site will be sporadically subjected to inputs of diluted river water, especially at spring tides during times of high river run-off.

The pattern of flow simulated by the model, and subsequently the predicted transport of freshwater to the coastal region, is dictated to a large extent by the Sound's channel system and the obstruction caused by the Breakwater. This gives rise to two separate flows either side of it, which run south and then turn west towards the Whitsand Bay area. This prediction highlights the importance of Tamar outflows to the water quality of the Whitsand Bay area, with some of the freshwater (and subsequently other material carried by the river waters) becoming temporarily trapped there. Even the most eastern release of tracer was transported offshore and then around Rame Head into the Whitsand Bay area. There have been anecdotal claims by divers of silt building up in Whitsand Bay; this work shows that this could be the result of a release of sediments into Plymouth Sound, the source of which could be dredging activity in the Tamar.

Recent events such as the grounding of the tanker 'Willy' and a dredging barge within the Sound, show that consideration must be given to the potential repercussions of such marine accidents. Only by having knowledge of the behaviour (both physical and biochemical) of any released materials can we hope to effectively predict and then minimize their effects upon local coastlines and ecosystems. Whitsand Bay would eventually receive, and due to the slow moving waters accumulate, a proportion of accidental releases within the Sound and should therefore be monitored for build up of contaminants, especially those associated with fine sediment.

This study was funded by the UK National Environmental Research Council (NERC) through the Plymouth Marine Laboratory core strategic research programme, Estuarine and Coastal Function and Health (ECoH). The authors are indebted to colleagues at Proudman Oceanographic Laboratory, especially Jason Holt and Roger Proctor who made the POL3DB model available for use at PML and provided invaluable advice on its use. The authors would also like to thank Peter Miller from the NERC Remote Sensing Data Analysis Service (RSDAS), who processed NOAA AVHRR satellite data received from Dundee Satellite Receiving Station for use in this work.

REFERENCES

Allen, J.I., Blackford, J., Holt, J.T., Proctor, R., Ashworth, M. & Siddorn, J.R., 2001. A highly spatially resolved ecosystem model for the North West European continental shelf. *Sarsia*, **86**, 423–440.

Biegala, I.C. & Harris, R.P., 1999. Sources of seasonal variability in mesozooplankton aspartate transcarbamylase activity in coastal waters off Plymouth, UK. *Journal of Plankton Research*, **21**, 2085–2103.

Budyko, M.I., 1974. *Climate and life*. New York: Academic Press.

Castellari, S., Pinardi, N. & Leaman, K., 1998. A model of air–sea interactions in the Mediterranean Sea, *Journal of Marine Systems*, **18**, 89–114.

Harris, J.R.W., Hamilin, C.C. & Stebbing, A.R.D., 1991. A simulation study of the effectiveness of legislation and improved dockyard practice in reducing TBT concentrations in the Tamar Estuary. *Marine Environmental Research*, **32**, 279–292.

Holt, J.T., James, I. & Jones, J.E., 2001. An *s* coordinate density evolving model of the northwest European continental shelf. 2. Seasonal currents and tides. *Journal of Geophysical Research*, **106**, 14 035–14 053.

Inglis J.C., 1877. Plymouth Sound: its tidal currents. *Journal of the Plymouth Institution*, **6**, 275–289.

Irigoien, X., Harris, R.P., Head, R.N. & Harbour, D., 2000. North Atlantic oscillation and spring bloom phytoplankton composition in the English Channel. *Journal of Plankton Research*, **22**, 2367–2371.

Kondo, J., 1975. Air–sea bulk transfer coefficients in diabatic conditions. *Boundary-Layer Meteorology*, **9**, 91–112.

Laabir, M., Poulet, S.A., Harris, R.P., Pond, D.W., Cueff, A., Head, R.N. & Ianora, A., 1998. Comparative study of the reproduction of *Calanus helgolandicus* in well-mixed and seasonally stratified waters of the western English Channel. *Journal of Plankton Research*, **20**, 407–421.

Mellor, G.L. & Yamada, T., 1974. A hierarchy of turbulence closure models for planetary boundary layers. *Journal of the Atmospheric Sciences*, **31**, 1791–1806.

Palma, E.D. & Matano, R.P., 2000. On the implementation of passive open boundary conditions for a general circulation model: the three-dimensional case. *Journal of Geophysical Research*, **105**, 8605–8627.

Pingree, R.D. & Griffiths, D.K., 1980. Currents driven by a steady uniform wind stress on the shelf seas around the British Isles. *Oceanologica Acta*, **3**, 227–236.

Proctor, R. & James, I.D., 1996. A fine resolution 3D model of the southern North Sea. *Journal of Marine Systems*, **8**, 285–295.

Ruddick, K.G., Deleersnijder, E., Luyten, P.J. & Ozer, J., 1995. Haline stratification in the Rhine–Meuse fresh water plume: a three-dimensional model sensitivity analysis. *Continental Shelf Research*, **15**, 12507–12630.

Siddorn, J.R. & Allen, J.I., 2002. Surface heat fluxes and ecosystem function in the Cretan Sea (Eastern Mediterranean): a modelling study. *Annales Geophysicae*, **20**, 1–12.

Sinha, B. & Pingree, R.D., 1997. The principal lunar semidiurnal tide and its harmonics: baseline solutions for M-2 and M-4 constituents on the North-West European continental shelf. *Continental Shelf Research*, **17**, 1321–1365.

Smith, S.D. & Banke, E.G., 1975. Variation of the sea surface drag coefficient with wind speed. *Quarterly Journal of the Royal Meteorological Society*, **101**, 665–673.

Uncles, R.J. & Stephens, J.A., 1990. Computed and observed currents, elevations, and salinity in a branching estuary. *Estuaries*, **13**, 133–144.

Submitted 11 February 2002. Accepted 1 May 2003.